Characterization of a [4Fe-4S]-dependent LarE sulfur insertase that facilitates nickel-pincer nucleotide cofactor biosynthesis in *Thermotoga maritima*

Shramana Chatterjee[1], Kristine F. Parson[2], Brandon T. Ruotolo[2], John McCracken[3], Jian Hu[3,4], and Robert P. Hausinger[1,4,*]

From the [1]Department of Microbiology and Molecular Genetics, Michigan State University, East Lansing, Michigan, USA; [2]Department of Chemistry, University of Michigan, Ann Arbor, Michigan, USA; [3]Department of Chemistry, and [4]Department of Biochemistry and Molecular Biology, Michigan State University, East Lansing, Michigan, USA

Edited by Wolfgang Peti

Sulfur-insertion reactions are essential for the biosynthesis of several cellular metabolites, including enzyme cofactors. In *Lactobacillus plantarum*, a sulfur-containing nickel-pincer nucleotide (NPN) cofactor is used as a coenzyme of lactic acid racemase, LarA. During NPN biosynthesis in *L. plantarum*, sulfur is transferred to a nicotinic acid–derived substrate by LarE, which sacrifices the sulfur atom of its single cysteinyl side chain, forming a dehydroalanine residue. Most LarE homologs contain three conserved cysteine residues that are predicted to cluster at the active site; however, the function of this cysteine cluster is unclear. In this study, we characterized LarE from *Thermotoga maritima* (LarE$_{Tm}$) and show that it uses these three conserved cysteine residues to bind a [4Fe-4S] cluster that is required for sulfur transfer. Notably, we found LarE$_{Tm}$ retains all side chain sulfur atoms, in contrast to LarE$_{Lp}$. We also demonstrate that when provided with L-cysteine and cysteine desulfurase from *Escherichia coli* (IscS$_{Ec}$), LarE$_{Tm}$ functions catalytically with IscS$_{Ec}$ transferring sulfane sulfur atoms to LarE$_{Tm}$. Native mass spectrometry results are consistent with a model wherein the enzyme coordinates sulfide at the nonligated iron atom of the [4Fe-4S] cluster, forming a [4Fe-5S] species, and transferring the noncore sulfide to the activated substrate. This proposed mechanism is like that of TtuA that catalyzes sulfur transfer during 2-thiouridine synthesis. In conclusion, we found that LarE sulfur insertases associated with NPN biosynthesis function either by sacrificial sulfur transfer from the protein or by transfer of a noncore sulfide bound to a [4Fe-4S] cluster.

The biological interconversion of chemical isomers or enantiomers is of fundamental importance to the metabolism of living organisms and has many applications in biocatalysis, biotechnology, and drug discovery (1). Depending on their substrates, isomerases are divided into four subclasses that act on amino acids and derivatives, α-hydroxyacids and derivatives, carbohydrates and derivatives, and other substances. The isomerization of D/L-lactate is catalyzed by lactate racemase (Lar), an enzyme that, in *Lactobacillus plantarum*, is a combination of the LarA protein and a tethered nickel-pincer nucleotide (NPN) cofactor (2). Homologs of LarA use NPN to catalyze racemization and epimerization reactions of a variety of α-hydroxy acid compounds other than lactate (3).

The biosynthesis of the NPN cofactor in *L. plantarum* requires three proteins that are encoded with LarA in the *lar* operon (Fig. 1) (4, 5). LarB is a carboxylase/hydrolase of nicotinic acid adenine dinucleotide (NaAD), forming pyridinium-3,5-biscarboxylic acid mononucleotide (P2CMN) (6). LarE sequentially converts the two carboxylic acids of P2CMN into thiocarboxylic acids, producing first pyridinium-3-carboxy-5-thiocarboxylic acid mononucleotide (PCTMN) and then pyridinium-3,5-bisthiocarboxylic acid mononucleotide (P2TMN) (7). Finally, LarC installs the nickel atom into P2TMN to generate NPN with the metal bonded in a planar arrangement by one carbon and two sulfur atoms of the coenzyme (8). The organometallic cofactor binds to *L. plantarum* LarA with its nickel coordinating His200 and by a thioamide linkage with Lys184. Analogous histidinyl and lysyl residues are found in other LarA homologs; however, NPN is not covalently attached to all proteins with which it associates.

This work focuses on the biosynthetic reaction catalyzed by LarE. Bioinformatics analysis reveals that LarE is a member of the PP-loop pyrophosphatase family that contains a PP-loop SGGXDS motif in its N-terminal region (9). This motif is responsible for catalyzing the ATP-dependent adenylylation of one P2CMN carboxyl group, with the activated intermediate undergoing sulfur transfer to form PCTMN, then a second round of adenylylation and sulfur transfer provides P2TMN. For LarE from *L. plantarum* (LarE$_{Lp}$) the sulfur originates from a cysteine residue (Cys176) of the protein, resulting in the formation of a dehydroalanine residue in LarE$_{Lp}$, making it a sacrificial sulfur transferase (7) (Fig. 2). LarE$_{Lp}$ is structurally related to other ATP-dependent sulfur transferases that contain [4Fe-4S] clusters or that generate persulfides at their active sites, such as TtuA, MnmA, and ThiI (10). Therefore, we speculated that other LarE homologs may bind a [4Fe-4S]

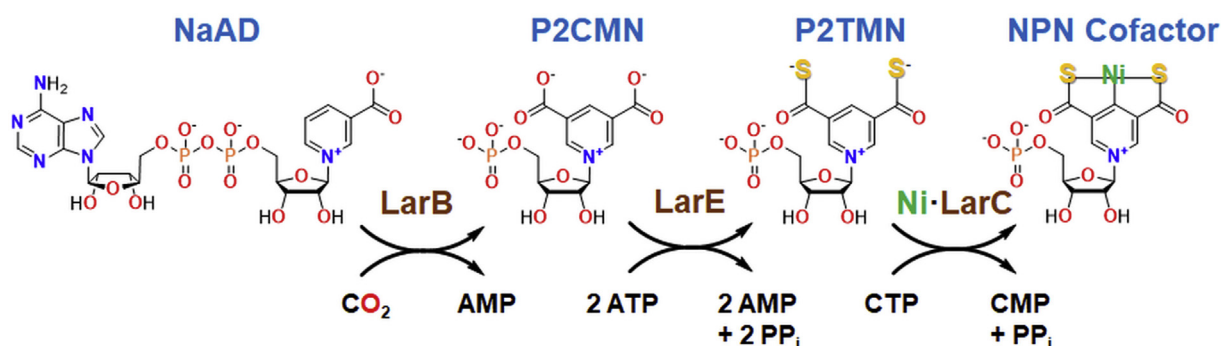* For correspondence: Robert P. Hausinger, hausinge@msu.edu.

Figure 1. Biosynthesis of the NPN cofactor. LarB carboxylates the pyridinium ring and hydrolyzes the phosphoanhydride linkage of nicotinic acid adenine dinucleotide (NaAD) to form pyridinium-3,5-biscarboxylic acid mononucleotide (P2CMN). LarE catalyzes the ATP-dependent conversion of P2CMN into pyridinium-3,5-bisthiocarboxylic acid mononucleotide (P2TMN). LarC inserts nickel into P2TMN to produce the NPN cofactor in a CTP-dependent reaction.

cluster or generate a persulfide instead of using an active site cysteine residue for catalytic sulfur transfer.

In this study, we identify LarE from *Thermotoga maritima* (LarE$_{Tm}$) as a [4Fe-4S] cluster-containing enzyme that coordinates the cluster using three cysteine residues. This conclusion is based on a combination of UV-visible (UV-vis) absorption and electron paramagnetic resonance (EPR) spectroscopies coupled with iron and sulfide analyses as well as

site-directed mutagenesis. In addition, we used *in vitro* enzyme assays to demonstrate that the cluster of LarE$_{Tm}$ is essential for its sulfur transferase activity. Unlike LarE$_{Lp}$, LarE$_{Tm}$ does not sacrifice a cysteinyl sulfur atom during catalysis. Rather, we show the [4Fe-4S] cluster is used to catalyze multiple rounds of sulfur transfer when provided with L-cysteine in the presence of cysteine desulfurase from *Escherichia coli* (IscS$_{Ec}$). We used mass spectrometry (MS) studies to reveal that IscS$_{Ec}$
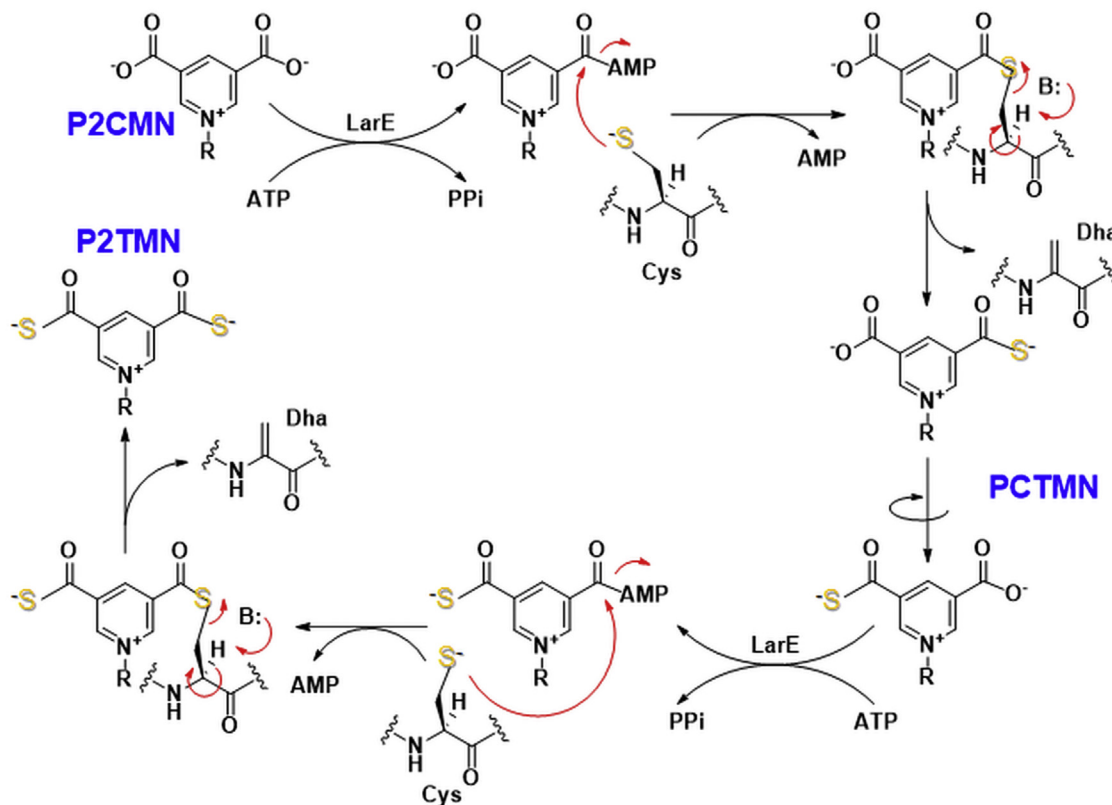

Figure 2. LarE$_{Lp}$ catalyzed biosynthesis of P2TMN from P2CMN. One carboxyl group of P2CMN is adenylylated to provide an activated substrate that is attacked by a cysteinyl residue of the enzyme, forming a covalent adduct. Transfer of the enzyme sulfur atom generates protein that contains dehydroalanine (Dha) while producing pyridinium-3-carboxy-5-thiocarboxylic acid mononucleotide (PCTMN). Another subunit of the enzyme then activates PCTMN, forming a covalent adduct. Subsequent sacrifice of the cysteinyl sulfur atom forms P2TMN and a second Dha-containing protein subunit. P2CMN, pyridinium-3,5-biscarboxylic acid mononucleotide; P2TMN, pyridinium-3,5-bisthiocarboxylic acid mononucleotide.

can directly transfer sulfane sulfur to LarE$_{Tm}$. From these results, we speculate that LarE$_{Tm}$ uses three conserved cysteines of the enzyme to bind the [4Fe-4S] cluster and coordinates a noncore sulfur atom at the fourth iron site, with the additional sulfur atom used to attack the activated substrate for sulfur transfer. This novel mechanism for LarE$_{Tm}$ resembles the sulfur-insertion reactions of thionucleotide-tRNA biosynthetic enzymes that also use tricoordinated [4Fe-4S] clusters to transfer a noncore sulfide (11, 12).

Results

Sequence analysis suggests that most LarE homologs possess a tri-Cys-bound iron-sulfur cluster

We analyzed sequences of LarE from selected bacteria and archaea (Fig. S1) and found that most homologs contain two conserved motifs: SGGXDS (P-loop motif, shown beneath the *green rectangular box*) and two cysteines in a CXXC sequence with another cysteine located more distantly (*i.e.*, the CXXC-C motif, shown beneath the *blue rectangular boxes*). In addition, a fourth cysteine residue is located adjacent to the CXXC-C motif in LarE sequences from *T. maritima*, *Ignisphaera aggregans*, and *Deltaproteobacteria bacterium* (shown by the *yellow star*), whereas the other sequences possess Ala, Ser, or Leu at this position. From the structure of LarE$_{Lp}$ in complex with Mg·ATP (Protein Data Bank ID: 5UDS), we know the SGGXDS motif (9) is responsible for binding ATP, which is essential for activity (7). The LarE$_{Tm}$ and LarE$_{Lp}$ sequences both contain the SGGXDS motif, but LarE$_{Lp}$ lacks the CXXC-C motif (Fig. 3). Moreover, a single residue shift occurs when comparing the active site Cys176 of LarE$_{Lp}$ to the third conserved Cys residue of the CXXC-C motif in LarE$_{Tm}$. We used Alphafold2 (13) to build a homology model of LarE$_{Tm}$ (Fig. 4A) that reveals a clustering of the four cysteine residues (Fig. 4B). Ser180, Arg212, and Arg214 of LarE$_{Lp}$ are proposed to bind the phosphate of the substrate P2CMN; these residues are conserved in LarE$_{Tm}$, so P2CMN is likely to bind in a similar manner. Significantly, the clustering of the three conserved cysteine residues is reminiscent of the situation for other PP-loop pyrophosphatase family members that catalyze sulfur transfer reactions using tricoordinated iron-sulfur clusters (10). Thus, we speculated that LarE homologs containing CXXC-C motifs, including that from *T. maritima*, bind Fe-S clusters, which participate in their sulfur transferase reactions, thus avoiding the need to forfeit the sulfur atom of a thiolate side chain.

LarE$_{Tm}$ does not sacrifice a cysteinyl sulfur atom

His$_6$-tagged LarE$_{Tm}$ was isolated from *E. coli* and shown by electrospray ionization-MS (ESI-MS) to have a mass of 31,732 Da, consistent with the expected size of 31,739 Da (Fig. S2). The enzyme was reacted with ATP, MgCl$_2$, and P2CMN (produced by incubation of LarB with NaAD and bicarbonate), as previously described (8). The His$_6$-tagged LarE$_{Tm}$ from the reaction mixture was directly examined by ESI-MS or characterized after further purification as described earlier (5). The mass of the protein remained constant throughout the reaction time, indicating that LarE$_{Tm}$ does not sacrifice a cysteinyl sulfur atom during the reaction to produce P2TMN (Fig. S2). By contrast, we used the same approach to confirm that LarE$_{Lp}$ catalyzed the previously reported sacrificial sulfur transfer reaction (5). The ESI-MS results for His$_6$-tagged LarE$_{Tm}$ also confirm the homogeneity of the sample. Analysis by size-exclusion chromatography-multiangle light scattering demonstrated that the protein exists as dimer ($M_r = 61,130 \pm 36$ Da) in solution (Fig. S3).

LarE$_{Tm}$ possesses an oxygen-labile [4Fe-4S] cluster

The aerobically purified protein (subunit concentration of 160 μM) was brownish in color (Fig. 5A), but the intensity of the broad absorption (maximum at ∼410 nm) decreased with time when exposed to air (Fig. 5B). When aerobically purified His$_6$-tagged LarE$_{Tm}$ (200 μM) was anaerobically incubated with iron and L-cysteine in the presence of IscS$_{Ec}$ (*i.e.*, cluster assembly conditions), the brownish color and the broad shoulder at 410 nm were greatly increased in intensity (Fig. 5C), consistent with an enhanced amount of cluster compared to the starting sample with its partially occupied metallocenter. The spectrum of anaerobic cluster-assembled LarE$_{Tm}$ (Fig. 5D) differed from that of the aerobically purified protein (Fig. 5B), presumably because the aerobic sample possessed some damaged cluster (*e.g.*, [3Fe-4S], [2Fe-2S], and perhaps other species). Anaerobic addition of sodium dithionite into cluster-assembled LarE$_{Tm}$ (400 μM) bleached the protein color and greatly diminished the UV-vis absorption (Fig. 5D). Inductively coupled plasma-optical emission spectroscopy (ICP-OES) revealed 4.1 ± 0.2 Fe atoms per subunit, and chemical analysis indicated the presence of 3.9 ± 0.2 inorganic sulfur atoms per monomer for protein that was analyzed after *in vitro* cluster assembly. These values are consistent with the presence of a [4Fe-4S] cluster in each subunit. We investigated the oxidation state properties of the


```
              1                                                  50                                                      100
L. plantarum  MATLATKKATLVAALKDLQRVTVAF SGGIDS TLVLKMALDVLGRDNVTAVVANSELFTDEEFDKAMSLAEEELGANVQGTTLDYLSDDHIKNNTPDSWYYAK
T. maritima   MDKLQRISEAIKSKKKLVVMF SGGVDS TLLAKLAREVLG-KNAVALTIDSPVIPRKEIEEAKNLANLIGIRHEFIELNELKSRHLIENPPDR CYLC R

              150                             176                              200
L. plantarum  KMFYSRLNDIAANNGSAAVLDGMIKNDENDYRPGLKARSEAGARSLLQEADFFKTDVRALAQELGLTNWNKVAS C SVSSRFPYGTTLTHDNIAQVMAAEKYLR
T. maritima   KLRDNIVKNWARENGFDVIADGLNFSDLQDYRPGVKASTEDGIWHPFIDFEVTKEEIREYSKKLGLPTWDKPAMA CLC SRFPYGFGLNEERVRMVEKAENFLR

              205                                    277
L. plantarum  SLGFPTVRVRFHN-DIARIELPEARIGDFL--VFNDRVNRQLQSLGFRYVTLDLGGFRSGRMNDTLTKAQLATFA
T. maritima   ELGFREVRVRFFPYKTAVVEVGRDEMELLMGK--RTDIVLALQKIGFSFVTLDLEGFASGKLNRTIEGMSK
```

Figure 3. Sequence comparison of LarE$_{Lp}$ and LarE$_{Tm}$. The *green* and *cyan highlights* are the motifs depicted by *green* and *blue* segments in Fig. S1. The sulfur-donating cysteine residue of LarE$_{Lp}$ is highlighted in *red*. The fourth cysteine residue adjacent to the CxxC-C motif in LarE$_{Tm}$ is highlighted in *yellow*. LarE$_{Lp}$, LarE from *Lactobacillus plantarum*; LarE$_{Tm}$, LarE from *Thermotoga maritima*.
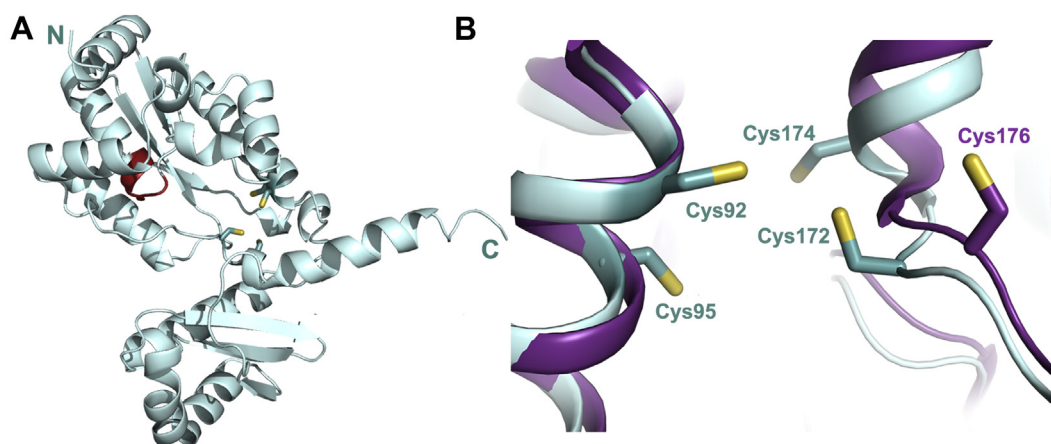
Figure 4. Homology model of LarE$_{Tm}$. *A*, cartoon depiction of the LarE$_{Tm}$ subunit model with the amino and carboxyl termini indicated (N and C, respectively), the PP-loop shown in *red*, and the four cysteine residues illustrated as *sticks*. *B*, comparison of the 4-cysteine cluster in the LarE$_{Tm}$ homology model (*light teal*) *versus* the corresponding region of LarE$_{Lp}$ (*purple*) that contains a single cysteine residue. LarE$_{Tm}$, LarE from *Thermotoga maritima*.

[4Fe-4S] cluster in cluster-assembled LarE$_{Tm}$ by EPR spectroscopy. The initial spectrum displayed low intensity signals near *g* ~2 at 10 K that are consistent with a small amount of the [4Fe-4S] cluster having been damaged and oxidized to form a [3Fe–4S]$^{1+}$ cluster and radicals (14). After treatment of the LarE$_{Tm}$ sample with low concentrations of sodium dithionite, we obtained an EPR spectrum (Fig. 6) with $g_{\parallel}$ = 2.02 and $g_{\perp}$ = 1.92, consistent with a [4Fe-4S]$^{+1}$ cluster (15), along with sharp radical signal (*g* = 2.00) that we attribute to unreacted SO$_2^{\cdot-}$ or a secondary radical (16, 17).

The [4Fe-4S] cluster of LarE$_{Tm}$ is required for its sulfur transferase activity

In the presence of Mg·ATP, freshly purified LarE$_{Tm}$ transformed P2CMN into PCTMN and P2TMN, as detected by selected ion monitoring during liquid chromatography (LC)-ESI-MS (Fig. 7). This enzyme activity was lost after oxygen exposure. The activities of LarE$_{Tm}$ samples also were assessed by using an indirect assay that involved the conversion of NaAD to P2CMN by LarB, LarE-catalyzed anaerobic transformation of this substrate to P2TMN, synthesis of NPN from

P2TMN by LarC, incorporation of the cofactor into LarA apoprotein from *Thermoanaerobacterium thermosaccharolyticum* (LarA$_{Tt}$), and measurement of the resulting Lar activity (Fig. 8A). Anaerobic cluster-assembled LarE$_{Tm}$ exhibited the greatest activity, whereas significantly reduced levels were observed for anaerobically purified protein, and essentially no activity was detected by this assay in the aerobically purified sample. To further characterize the reaction, we examined different time intervals (Fig. 8B) as well as different concentrations of the cluster-assembled LarE$_{Tm}$ (Fig. 8C). We observed increasing levels of activity for the first 10 min of the reaction, but longer time periods led to a small reduction of activity. As expected, using larger amounts of LarE$_{Tm}$ led to greater levels of Lar activity; however, a linear dependence was not observed. As a means to potentially allow catalytic, rather than stoichiometric, activity of LarE$_{Tm}$, we provided exogenous sulfur sources. Treating LarE$_{Tm}$ with L-cysteine and His$_6$-tagged IscS$_{Ec}$ provided a substantial increase in the levels of Lar activity (Fig. 8D). In contrast, provision of Na$_2$S as an external sulfur source along with FeCl$_3$ did not increase the level of Lar activity over the control (Fig. 8E). These results suggest that LarE$_{Tm}$ can use L-cysteine as sulfur donor when
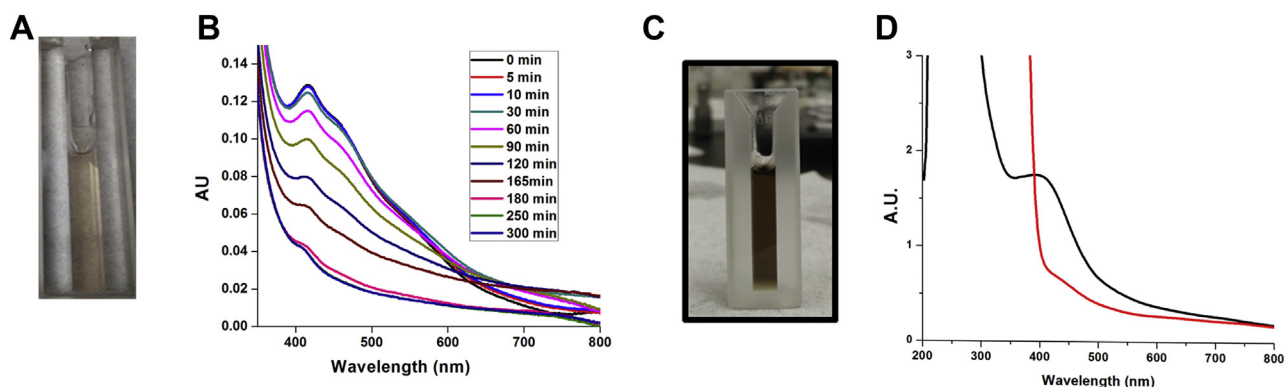

Figure 5. UV-visible spectroscopy indicates the presence of an oxygen-labile and redox-active [Fe-S] cluster in His$_6$-tagged LarE$_{Tm}$. *A*, aerobically purified LarE$_{Tm}$ (160 μM subunit concentration) was *brownish* in color. *B*, the spectrum of LarE$_{Tm}$ decreased in intensity when incubated in air up to 300 min. *C*, aerobically purified LarE$_{Tm}$ (200 μM) that had been subjected to cluster assembly conditions yielded a much more intense *brown* spectrum. *D*, the addition of Na$_2$S$_2$O$_4$ (8 mM) to the cluster-assembled LarE$_{Tm}$ led to a bleaching of the spectrum (*black* to *red*). All samples were prepared in 100 mM Tris buffer at pH 7.2. LarE$_{Tm}$, LarE from *Thermotoga maritima*.
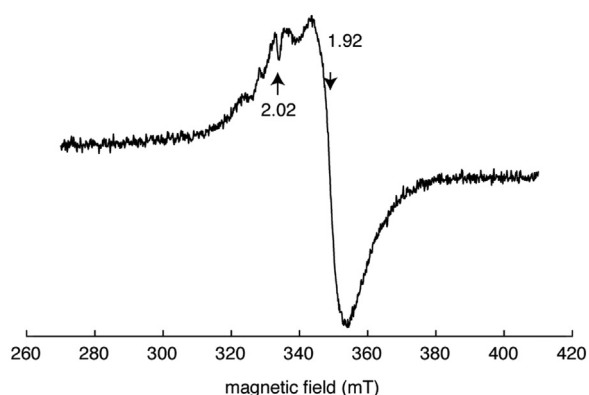
Figure 6. EPR spectrum of dithionite-reduced, cluster-assembled, His$_6$-tagged LarE$_{Tm}$. The spectrum was obtained under the following conditions: microwave frequency, 9.3941 GHz; microwave power, 0.25 mW; magnetic field modulation amplitude, 1.2 mT; sample temperature, 10 K. EPR, electron paramagnetic resonance; LarE$_{Tm}$, LarE from *Thermotoga maritima*.

provided along with His$_6$-tagged IscS$_{Ec}$, whereas Na$_2$S does not serve as the sulfur source for the sulfur transferase activity of this enzyme.

Mutational analysis of the cysteine codons of LarE$_{Tm}$

To further test the importance of the [4Fe-4S] cluster to the sulfur transferase activity of LarE$_{Tm}$, we mutated the gene to substitute each of its three conserved cysteine residues (Cys92, Cys95, and Cys172) with alanine. The three variant proteins were isolated aerobically, UV-vis absorption spectra were

acquired (Fig. 9*A*), the samples were subjected to cluster assembly conditions, the modified spectra were acquired (Fig. 9*B*), and the variants were measured for enzymatic activity (Fig. 9*C*). The broad absorption peak at ∼410 nm was decreased, but not eliminated, for each of the variants as initially purified in comparison to the control protein at the same concentration (100 μM). On the basis of the A$_{410}$/A$_{280}$ ratios of the C92A, C95A, and C172A variant proteins and comparison to the WT enzyme, the relative amounts of [4Fe-4S] cluster present were approximately 48%, 54%, and 61%, respectively (Fig. 9*A*). After treatment of the proteins with cluster-assembly conditions, the samples were much more closely matched in their 410 nm absorption with slightly less in the C92A variant (Fig. 9*B*). The enzymatic activities of the cluster-assembled C92A, C95A, and C172A variants (assayed at 7.5 μM concentrations) were 63%, 64%, and 71% of that for the WT enzyme using the Lar assay, respectively (Fig. 9*C*). These activity experiments were performed at least twice and were also reproduced at different assay time periods. The results are consistent with the Cys92, Cys95, and Cys172 residues being ligands of the [4Fe-4S] cluster but indicate that cluster formation and substantial activity is retained even when one of these ligands is removed. The sequence alignment and the LarE$_{Tm}$ homology model show the presence of a fourth cysteine residue (Cys174) adjacent to the tri-Cys cluster. To examine whether Cys174 participates in enzymatic activity and whether it might substitute for Cys172 when that residue is
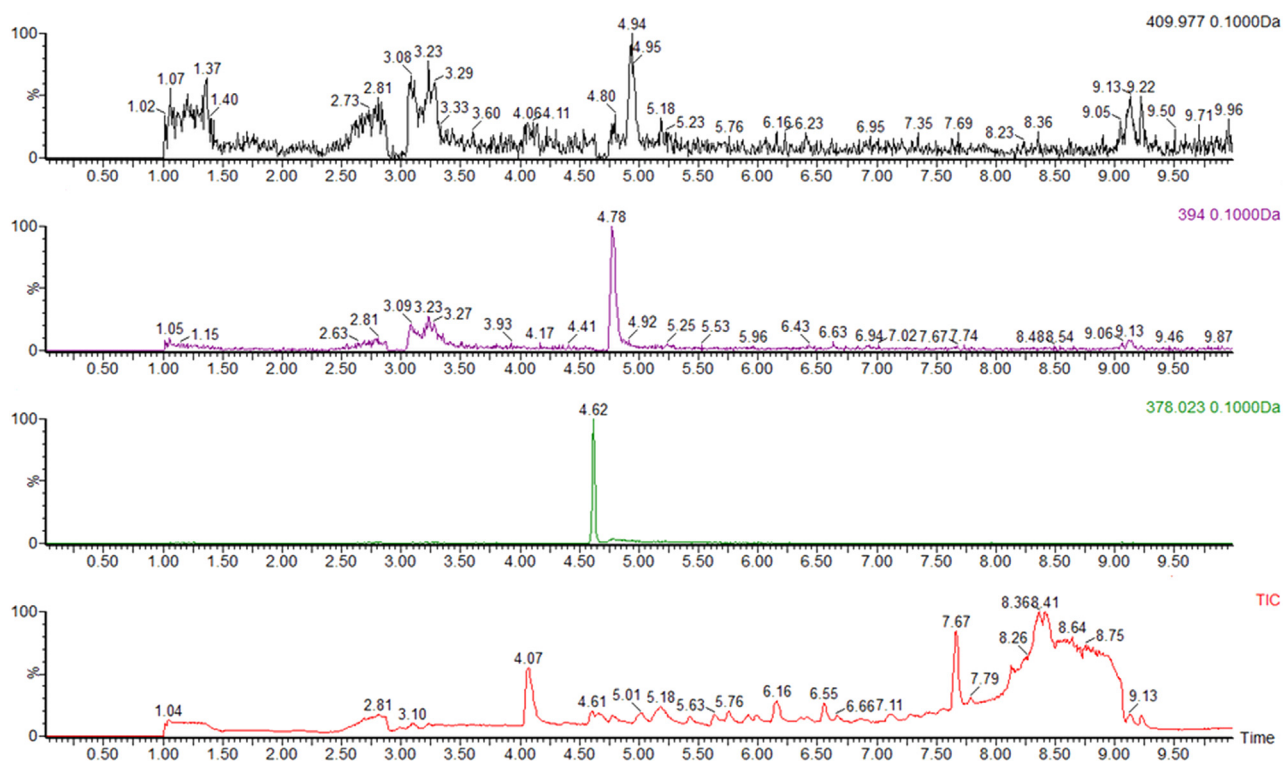

Figure 7. His$_6$-tagged LarE$_{Tm}$ converts P2CMN into PCTMN and P2TMN as shown by LC-ESI-MS chromatography. Selected ion monitoring of P2TMN (*top* scan at 410.0 Da), PCTMN (second scan at 394.0 Da), and P2CMN (third scan at 378.0 Da) elute at 4.94, 4.78, and 4.62 min, respectively. The *bottom panel* shows the total ion chromatogram (TIC). The reaction was performed using freshly purified LarE$_{Tm}$ (∼1 mM, isolated aerobically) in 100 mM Tris, pH 7.2 buffer containing 20 mM MgCl$_2$ and 2 mM ATP. ESI-MS, electrospray ionization-mass spectrometry; LarE$_{Tm}$, LarE from *Thermotoga maritima*; LC, liquid chromatography; P2CMN, pyridinium-3,5-biscarboxylic acid mononucleotide; P2TMN, pyridinium-3,5-bisthiocarboxylic acid mononucleotide; PCTMN, pyridinium-3-carboxy-5-thiocarboxylic acid mononucleotide.
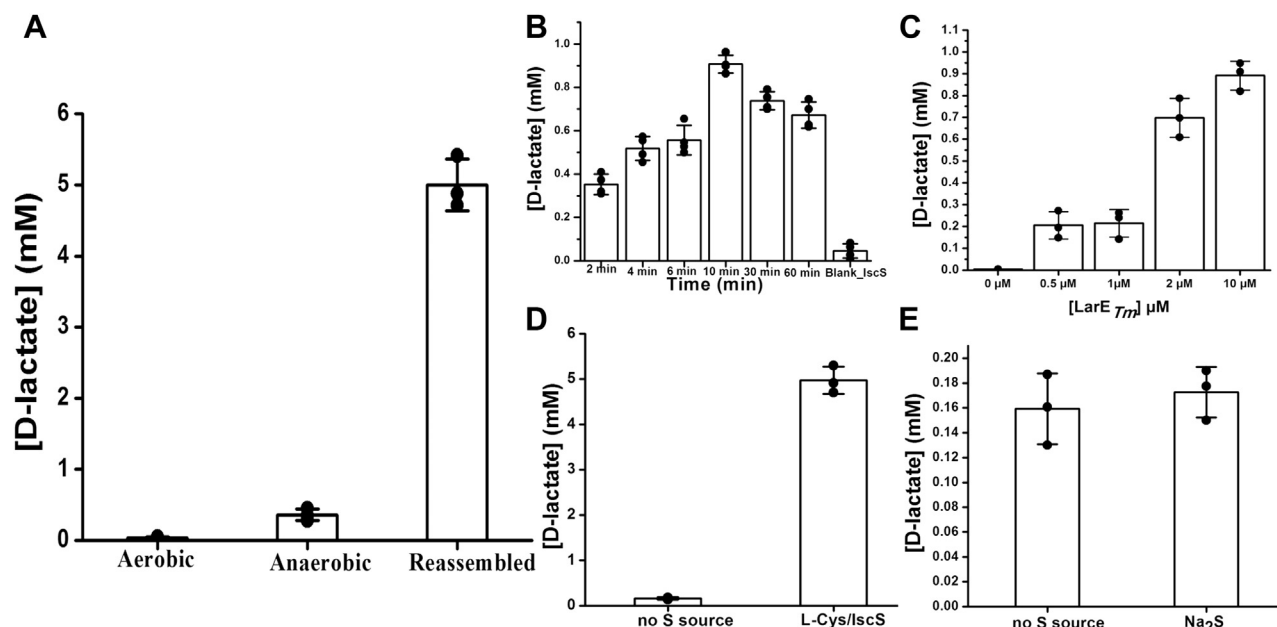
Figure 8. Sulfur transferase activity of His$_6$-tagged LarE$_{Tm}$. LarE$_{Tm}$ samples were incubated at room temperature for the indicated time periods with P2CMN (prepared by LarB$_{Lp}$-catalyzed transformation of NaAD), 20 mM MgCl$_2$, and 2 mM Mg·ATP, then denatured by heat treatment at 80 °C for 10 min. The activities of the LarE$_{Tm}$ samples were assessed by an indirect assay in which the LarE$_{Tm}$ product, P2TMN, was converted into NPN using LarC$_{Lp}$, the cofactor was incorporated into LarA$_{Tt}$ apoprotein, and Lar activity was monitored based on the production of D-lactate from 45 mM L-lactate in the starting solution. *A*, comparison of activities after 60 min incubation for three LarE$_{Tm}$ samples at 1 mM concentration: prepared aerobically, isolated anaerobically, and purified then subjected to anaerobic cluster-assembly conditions. *B*, time dependence of activity for cluster-assembled LarE$_{Tm}$ based on the subsequent conversion of P2TMN to NPN and activation of lactate racemase, monitoring D-lactate production. A low concentration of enzyme (10 μM) was used to allow for kinetic analysis. *C*, effect of the LarE$_{Tm}$ enzyme concentration on activity during 10 min of incubation as measured by the downstream Lar activity determination. *D*, effect of added L-Cys (10 mM) plus IscS$_{Ec}$ (20 μM) on the activity of LarE$_{Tm}$ (1 mM) compared to the activity of enzyme with no sulfur supplementation during a 10 min incubation, as monitored by the resulting Lar activity. *E*, effect of added Na$_2$S (10 mM) on the activity of LarE$_{Tm}$ (1 mM) compared to the activity of enzyme with no sulfur supplementation during a 10 min incubation, based on the observed Lar activity. The plots include individual data points, the means, and the SDs. LarE$_{Tm}$, LarE from *Thermotoga maritima*; NaAD, nicotinic acid adenine dinucleotide; P2CMN, pyridinium-3,5-biscarboxylic acid mononucleotide; P2TMN, pyridinium-3,5-bisthiocarboxylic acid mononucleotide.

altered, we created constructs that encode the C174A variant and the C172A/C174A double variant. As expected, C174A LarE$_{Tm}$ retained nearly all (84%) of the control protein activity, whereas the C172A/C174A protein possessed essentially the same Lar activity (59%) as the C172A single variant (Fig. 9C).

We conclude that Cys174 is not important for LarE$_{Tm}$ activity. To further examine the role of the conserved cysteine residues (Cys92, Cys95, and Cys172) we generated all possible combinations of double variants as well as the triple variant. Greatly diminished levels of activity were observed for the double
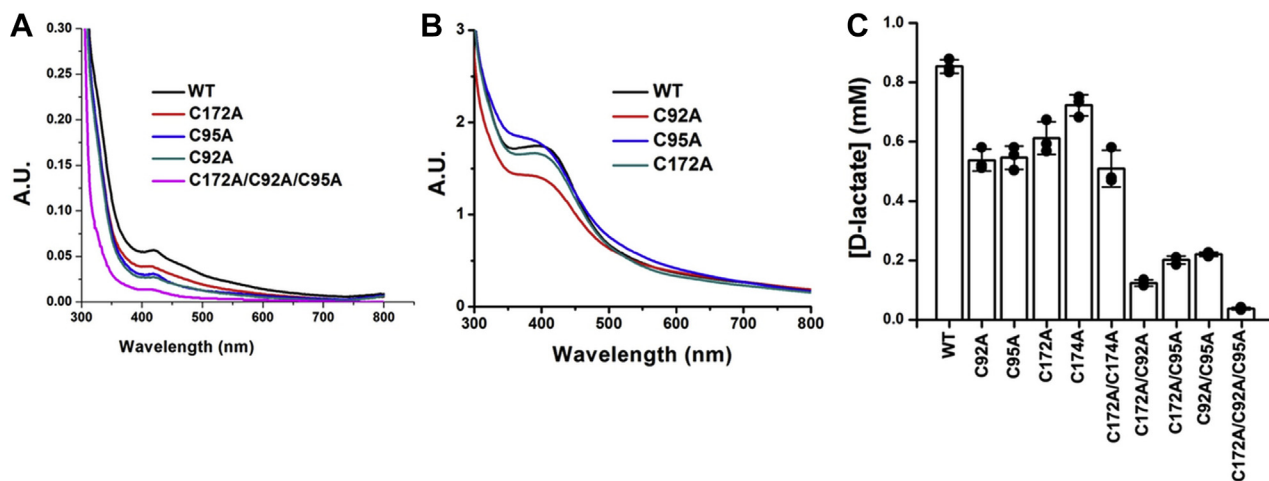

Figure 9. Mutational analysis of conserved cysteine codons of LarE$_{Tm}$. *A*, UV-visible spectra were acquired for the control His$_6$-tagged LarE (WT) and its C92A, C95A, C172A, and C172A/C92A/C95A variants (100 μM) immediately after purification. *B*, WT, C92A, C95A, and C172A variants were subjected to cluster-assembly conditions and the spectra acquired. *C*, WT LarE and combinations of cysteine variants (all at 7.5 μM) were incubated with P2CMN, 20 mM MgCl$_2$, and 2 mM Mg·ATP for 10 min and then examined for enzyme activity using the indirect Lar activation assay that monitors D-lactate production. This plot includes individual data points, the means, and the SDs. LarE$_{Tm}$, LarE from *Thermotoga maritima*.

variants (Fig. 9C). For the C92A/C95A/C172A variant, the broad absorption peak at ~410 nm (Fig. 9A) and the Lar activity (Fig. 9C) were nearly eliminated, confirming the critical role of these residues in LarE$_{Tm}$ activity.

Cysteine desulfurase can supply sulfur to LarE$_{Tm}$

As indicated previously, the inclusion of His$_6$-tagged IscS$_{Ec}$ and L-cysteine greatly enhanced the activity of His$_6$-tagged LarE$_{Tm}$ when assessed using the indirect Lar activation assay. This finding led us to consider whether IscS$_{Ec}$ may donate sulfur to LarE$_{Tm}$ for subsequent incorporation into the cofactor. Genes encoding two cysteine desulfurases (*tmari_1700* and *tmari_1378*) are located distant from that encoding LarE$_{Tm}$ (*tmari_0968*) in the *T. maritima* genome, with the product from *tmari_1700* (IscS$_{Tm}$) sharing 40% sequence identity with IscS$_{Ec}$ (155 matches out of 384 residues) (Fig. S4A). The crystal structure of IscS$_{Ec}$ (Protein Data Bank ID: 3LVK) (Fig. S4B) was used to create a homology model of IscS$_{Tm}$ (prepared by SWISS MODEL) (18) (Fig. S4C) that depicts the conserved position of a cysteine residue, which would accept sulfane sulfur from cysteine during the pyridoxal phosphate-dependent reaction (19). We used small molecule LC-MS analysis to explore whether IscS$_{Ec}$ can directly supply sulfur to LarE$_{Tm}$ for subsequent biosynthesis of the NPN cofactor in a manner similar to its reported roles during biosynthesis of other sulfur-containing cofactors such as iron-sulfur clusters, thiamin, and biotin (20–22). We incubated the cluster-assembled His$_6$-tagged LarE$_{Tm}$ (10 μM) with P2CMN, 20 mM MgCl$_2$, and 2 mM ATP for 60 min inside the anaerobic chamber at room temperature (RT), then added anoxic IscS$_{Ec}$ (100 μM) and L-cysteine (10 mM) for another 60 min. Equal volumes of buffer were added to a control sample (lacking L-cysteine and IscS$_{Ec}$) that was incubated for a total of 120 min. Analysis of the metabolites by LC-MS revealed a fourfold greater amount of P2TMN produced in the presence

of IscS$_{Ec}$ and L-cysteine (Fig. 10A). The results are shown as relative changes because no standards are available for P2CMN or P2TMN so the concentrations of substrate provided and product formed are not established. To confirm and extend this result, we varied the relative amount of P2CMN by adding one, two, and three equivalent volumes to the reactions during the 60 min incubation, while maintaining a constant concentration of LarE$_{Tm}$ (10 μM). The presence of IscS$_{Ec}$ and L-cysteine led to clear increases in P2TMN production as more P2CMN substrate was provided, whereas in their absence, the production of P2TMN was very low at all levels of P2CMN provided (Fig. 10B).

Direct donation of sulfane sulfur from the IscS$_{Ec}$ persulfide

The increase in the relative amount of P2TMN produced in the presence of IscS$_{Ec}$ and L-cysteine is consistent with a recycling of sulfur-depleted LarE$_{Tm}$ by sulfur transfer from an IscS$_{Ec}$ persulfide. We used an ESI-MS approach (23) to examine the mass changes of His$_6$-tagged IscS$_{Ec}$ during the postulated transfer of sulfane sulfur to LarE$_{Tm}$. The deconvoluted mass spectrum of as-purified His$_6$-tagged IscS$_{Ec}$ was comprised predominantly of the monomer molecular ion peak at 47,304 Da, along with a small peak at 47,339 Da and a slight feature at 47,374 Da (Fig. 11A). This spectrum is in excellent agreement with the theoretical mass (47,302.94 Da) for the IscS$_{Ec}$ sequence, which includes a linker to the His$_6$ tag, along with small amounts of sulfane sulfur bound to the protein as purified. After incubating the IscS$_{Ec}$ with excess L-cysteine for 60 min at RT and removing excess L-cysteine with a PD-10 desalting column, a large fraction of the sample had shifted in mass to molecular ion peaks at 47,336 Da and 47,369 Da (Fig. 11B). These changes represent increases of 32 and 65 Da and are consistent with additions of one and two sulfane sulfur atoms to the protein, forming the persulfide (IscS-S) and a larger species. The addition of a stoichiometric amount of
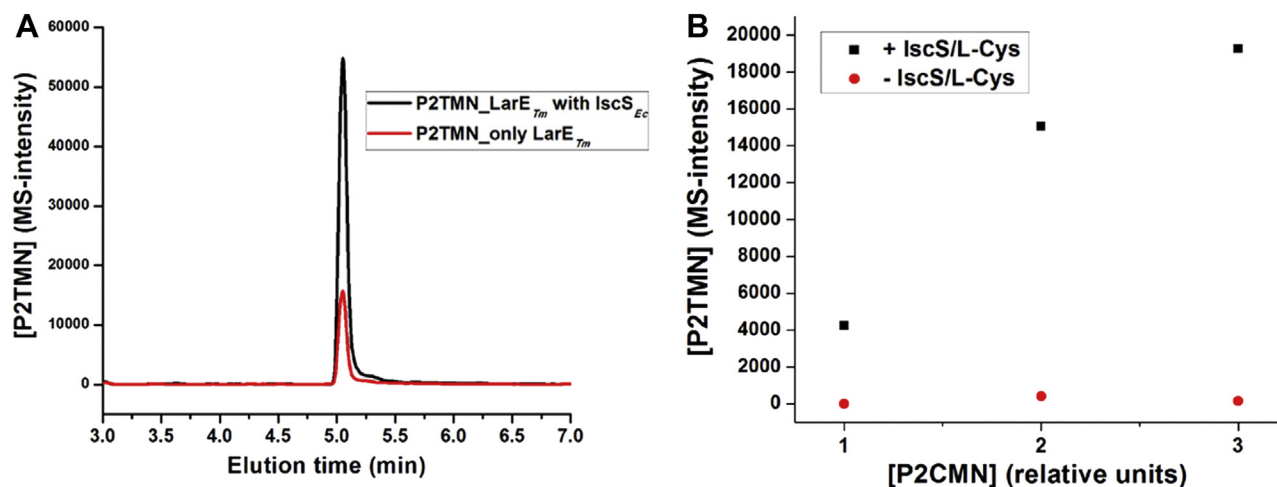

Figure 10. The relative amount of P2TMN produced by LarE$_{Tm}$ increases in the presence of IscS$_{Ec}$ and L-cysteine. *A*, the LC-MS intensity values of the P2TMN product were compared for His$_6$-tagged LarE$_{Tm}$ (10 μM) incubated with P2CMN, 2 mM ATP, and 20 mM MgCl$_2$ for 120 min (*red line*) versus an identical sample incubated with the same conditions for 60 min, followed by 60 min incubation with added His$_6$-tagged IscS$_{Ec}$ (100 μM) and L-cysteine (10 mM) (*black line*). *B*, similar P2TMN LC-MS intensity analyses were carried out for samples containing or lacking IscS$_{Ec}$ plus L-cysteine using three concentrations of substrate P2CMN (shown as relative units because a standard is not available for comparison) for a total incubation period of 120 min. IscS$_{Ec}$, cysteine desulfurase from *Escherichia coli*; LarE$_{Tm}$, LarE from *Thermotoga maritima*; P2CMN, pyridinium-3,5-biscarboxylic acid mononucleotide; P2TMN, pyridinium-3,5-bisthiocarboxylic acid mononucleotide.
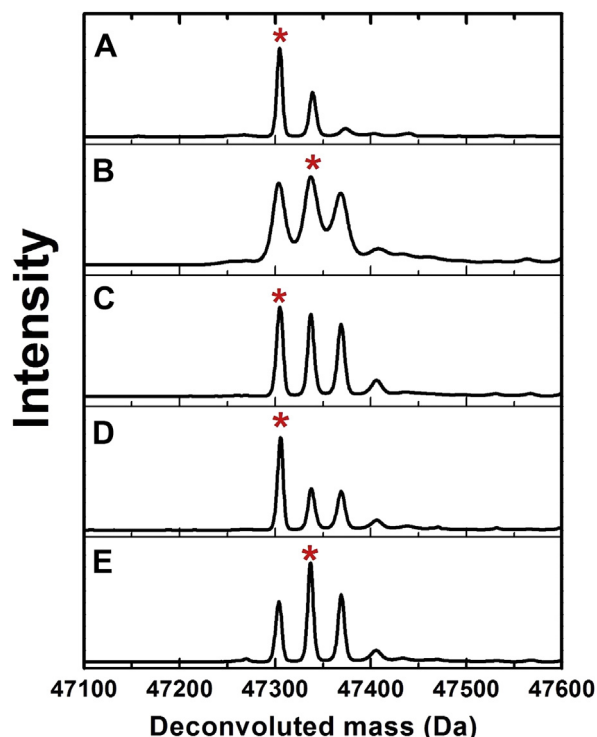
ASBMB

J. Biol. Chem. (2022) 298(7) 102131 **7**

Figure 11. Sulfane sulfur transfer from persulfidated IscS$_{Ec}$ to LarE. ESI-MS data were collected and the results deconvoluted for (*A*) as purified His$_6$-tagged IscS$_{Ec}$, (*B*) the purified IscS$_{Ec}$ treated with L-cysteine to produce the IscS with one or more added sulfane sulfur atom (IscS-S), (*C*) IscS-S incubated with aerobically-purified His$_6$-tagged LarE$_{Tm}$, (*D*) IscS-S incubated with anaerobically purified and cluster-assembled His$_6$-tagged LarE$_{Tm}$, and (*E*) IscS-S incubated with bovine serum albumin. The concentrations of IscS$_{Ec}$, LarE$_{Tm}$, and bovine serum albumin were each 10 µM and that of L-cysteine was 0.5 mM. Major peaks have been marked with *red stars*. ESI-MS, electrospray ionization-mass spectrometry; IscS$_{Ec}$, cysteine desulfurase from *Escherichia coli*; LarE$_{Tm}$, LarE from *Thermotoga maritima*.

aerobically purified His$_6$-tagged LarE$_{Tm}$ to this IscS-S sample led to a small shift in the proportions of the three species, increasing the relative amount of free IscS$_{Ec}$ (Fig. 11*C*). This shift was much more pronounced when adding a stoichiometric amount of anaerobically purified and cluster-assembled LarE$_{Tm}$ that possessed greater levels of intact [4Fe-4S] cluster (Fig. 11*D*). In contrast to these changes, the addition of a stoichiometric amount of bovine serum albumin had no effect on the molecular ion peaks in the sample containing IscS-S (Fig. 11*E*). These results suggest that persulfidated IscS$_{Ec}$ can catalyze direct transfer of sulfane sulfur to LarE$_{Tm}$. As the shift for IscS$_{Ec}$ is more pronounced upon incubation with cluster-assembled LarE$_{Tm}$ (Fig. 11*D*), it is reasonable to propose that sulfane sulfur has been transferred to the cluster.

Formation of a [4Fe-5S] cluster in LarE$_{Tm}$

The lability of the [4Fe-4S] cluster in His$_6$-tagged LarE$_{Tm}$ precluded use of the aforementioned denaturing ESI-MS method to assess whether sulfane sulfur adds to the *T. maritima* protein. Rather, we used nondenaturing nano–ESI-MS of cluster-assembled His$_6$-tagged LarE$_{Tm}$ after anaerobic incubation with IscS$_{Ec}$ and L-cysteine (Fig. 12). The native MS data reveal signals associated with dimer, tetramer, and

hexameric forms of LarE when using 15 eV for collision-induced dissociation (CID). When subjected to a CID energy of 100 eV, signals appear for what is assigned to the LarE monomer, as is typical for such data acquired for noncovalent protein complexes (24). By focusing our analysis on signals for the 15+ charge state of LarE dimers and the 12+ charge state of LarE monomers, we obtained the iron and sulfur stoichiometries associated with the subunits. For this analysis, the numbers of iron and sulfur atoms indicated within the brackets represent the numbers of these atoms bound per subunit and do not necessarily equate to the type of bound iron-sulfur cluster. The observed stoichiometries ranged from [Fe-S] to [4Fe-4S] for the LarE monomer and from [3Fe-4S][3Fe-4S] to [5Fe-5S][5Fe-5S] for LarE dimers (Fig. 12 and Tables S1 and S2). It is possible that the high CID energies required to initiate monomer ejection from the complexes interrogated here resulted in some loss of iron and sulfur from the LarE monomers, giving rise to the lower stoichiometries in these species when compared to the LarE dimer. In addition, it is plausible that iron released from damaged clusters binds adventitiously to some subunits, accounting for subunits associated with five metal ions.

The native MS data revealed prominent peaks that are increased in mass by 384 Da with respect to the apoprotein. A [4Fe-4S] cluster possesses a mass of 352 Da (25), which is also detected, so the 384 Da mass shift is suggestive of a sulfide bound to such a cluster forming a [4Fe-5S] species. We propose that the dimer species labeled [4Fe-4S][4Fe-4S] and [4Fe-5S][4Fe-5S] contain these types of clusters in the two subunits. Additionally, we suggest that dimer species labeled [4Fe-5S][5Fe-5S] and [5Fe-5S][5Fe-5S] each contain two copies of the [4Fe-5S] cluster with adventitious iron atoms bound to one or two of the subunits. We recognize that as an alternative to a [4Fe-5S] cluster, subunits containing a [4Fe-4S] cluster and a cysteine persulfide cannot be ruled out (25).

Discussion

We have provided evidence that the sulfur transferase activity of LarE$_{Tm}$ requires the presence of a [4Fe-4S] cluster that is tricoordinated by three cysteine residues. The cluster is oxygen labile and the protein cluster-binding site is only fully occupied when LarE$_{Tm}$ is subjected to cluster-assembly conditions. The labile nature of the cluster results in the EPR spectroscopic detection of small amounts of oxidized [3Fe–4S]$^{1+}$ cluster in the anaerobically purified enzyme, conditions when most of the protein contains diamagnetic [4Fe-4S]$^{2+}$ metallocenter, whereas a more intense spectrum is generated in the reduced sample due to a [4Fe-4S]$^{1+}$ state. Of interest, the presence of a [4Fe-4S] cluster in LarE$_{Tm}$ resembles the situation for TtuA, a sulfur transferase involved in 2-thiouridine biosynthesis that binds its cluster using three cysteine residues (26–28).

Our analysis of LarE$_{Tm}$ variants confirms the requirement of Cys92, Cys96, and Cys172, but not Cys174, for coordinating the [4Fe-4S] cluster and conferring activity. Individual substitutions of the cluster ligands reduce the amount of cluster in aerobically purified enzyme samples, but when subjected to cluster assembly conditions, the variant proteins exhibit nearly
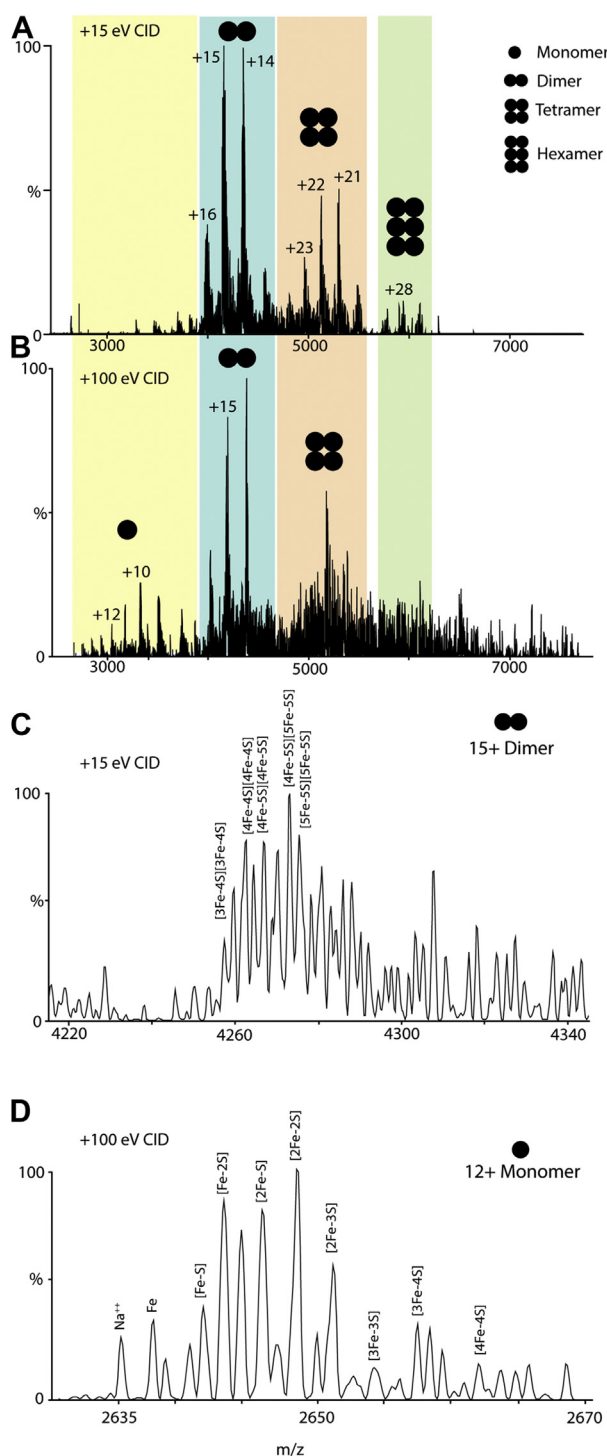
Figure 12. Native mass spectrometry of LarE$_{Tm}$. The figure illustrates the abundance of LarE$_{Tm}$ with bound iron and sulfur atoms. *A*, when using a CID of 15 eV, the dimer, tetramer, and hexamer oligomeric states are observed, but the spectrum is void of monomeric signals. *B*, using a CID of 100 eV, the monomeric species becomes evident. *C*, focusing on the 15+ charge state of the dimeric species, multiple Fe-S stoichiometries are observed. *D*, at the *high* CID energy of 100 eV, Fe-S stoichiometries are recorded for the 12+ charge state of monomeric LarE$_{Tm}$. LarE$_{Tm}$, LarE from *Thermotoga maritima*; CID, collision-induced dissociation.

full incorporation of the cluster according to the intensity of the UV-vis spectra. Furthermore, the activity of these single cysteine variant proteins was only modestly reduced compared

to the native protein. Double cysteine variants of LarE$_{Tm}$ are more greatly affected and only the triple cysteine variant fails to acquire a cluster or exhibit activity. Somewhat analogous results have been observed for other proteins; for example, variants of the HBx protein of hepatitis B virus where single substitution of cluster ligands did not affect cluster incorporation, and complete abolishment of cluster binding required substitution of all ligands (29).

In the presence of IscS$_{Ec}$ and L-cysteine, the activity of LarE$_{Tm}$ dramatically improves, consistent with donation of sulfane sulfur from IscS$_{Ec}$ to LarE$_{Tm}$. Indeed, we used ESI-MS analyses to demonstrate that the persulfide sulfur atom of IscS$_{Ec}$ is significantly lost only when incubated with the [4Fe-4S]-containing form of LarE$_{Tm}$ but not with the cluster-free protein or with the control protein bovine serum albumin. Furthermore, analysis of the resulting sample by anaerobic, nano–ESI-MS provided evidence consistent with the formation of LarE$_{Tm}$ possessing a [4Fe-5S] cluster, although a [4Fe-4S] cluster plus a persulfide cannot be ruled out. Surprisingly, the native LarE$_{Tm}$ MS study revealed peaks for the dimer, tetramer, and hexamer species. The crystal structure of LarE$_{Lp}$ reveals a hexamer that forms by head-to-head interaction of two trimers (7). The lack of a trimeric species for LarE$_{Tm}$ may indicate that it has a distinct quaternary structure.

We propose that a persulfide sulfur atom on IscS$_{Ec}$ transfers to the open iron coordination site on the [4Fe-4S] cluster of LarE$_{Tm}$ as a noncore sulfide atom (Fig. 13). Formation of this [4Fe-5S] cluster would presumably require additional reductant, available from the excess L-cysteine in the activation mixture. We further propose that the cluster-coordinating sulfide attacks the adenylylated P2CMN, formed *via* the same reaction as that catalyzed by LarE$_{Lp}$, to produce PCTMN and AMP. A second round of sulfur transfer from the IscS$_{Ec}$ persulfide to the [4Fe-4S] cluster of LarE$_{Tm}$ regenerates the [4Fe-5S] cluster that reacts with activated PCTMN to form P2TMN. Significantly, this mechanism avoids the conversion of a cysteinyl residue into a dehydroalanine side chain as seen in LarE$_{Lp}$. We verified by ESI-MS the retention of all cysteinyl sulfur in LarE$_{Tm}$ and its loss from LarE$_{Lp}$. It is remarkable that the same overall protein architecture is used for two such distinct mechanisms for transferring sulfur into P2CMN to make P2TMN.

Our demonstration of two distinct LarE sulfur-transfer mechanisms for the biosynthesis of the NPN cofactor has a clear parallel in the two reactions used for sulfur insertion during tRNA thionucleotide synthesis (11, 12). One thiobase-forming mechanism is exemplified by 4-thiouridine synthesis involving the initial activation of the precursor nucleotide using an adenylyltransferase followed by action of a sulfur transferase that catalyzes persulfide attack on the intermediate with release of AMP (30–32). A second thionucleotide-forming mechanism is associated with [Fe-S] cluster-containing enzymes that resemble LarE$_{Tm}$. An early study showed that *E. coli* catalyzes C2 thiolation of cytosine in tRNA using an enzyme that contains an essential, but oxygen labile, cluster (33). A mechanism involving sulfur transfer of a noncubane sulfide ligand was postulated but not demonstrated. A report
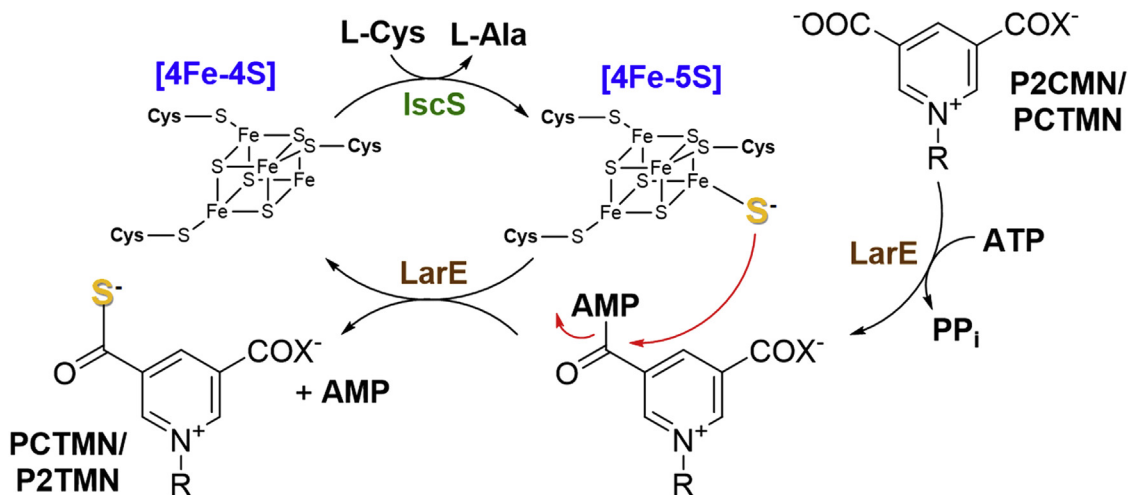
Figure 13. Proposed mechanism of LarE_{Tm}. We hypothesize that LarE_{Tm} activates P2CMN or PCTMN by adenylylation (*right portion* of the scheme), in the same manner as demonstrated for the LarE_{Lp} protein. Rather than sacrificing a cysteinyl sulfur atom, however, LarE_{Tm} attacks the activated substrate using a noncore sulfide bound to the open iron site in a tricoordinated [4Fe-4S] cluster, that is, a [4Fe-5S] cluster. The resulting [4Fe-4S]-containing enzyme species lacking the noncore sulfide is restored to the active species by acquiring a sulfane sulfur atom provided from an IscS persulfide that transiently forms as it catalyzes its cysteine desulfurase activity. Two rounds of this mechanism are required to convert P2CMN to P2TMN. LarE_{Tm}, LarE from *Thermotoga maritima*; P2CMN, pyridinium-3,5-biscarboxylic acid mononucleotide; P2TMN, pyridinium-3,5-bisthiocarboxylic acid mononucleotide; PCTMN, pyridinium-3-carboxy-5-thiocarboxylic acid mononucleotide.

describing enzymes used for synthesis of tRNA containing 2-thiouridine or 4-thiouridine in *Methanococcus maripaludis* and of 2-thiouridine in eukaryotes suggested they possess [3Fe-4S] clusters (34), but later a case was made that these enzymes contain oxygen-labile [4Fe-4S] clusters (11). The 4-thiouridine tRNA synthase from *M. maripaludis* uses exogenous sulfide as a sulfur source (34), consistent with an extra cubane-associated sulfide. Synthesis of 5-methyl-2-thiouridine in the tRNA of *Thermus thermophilus* involves two proteins: TtuA contains a PP-loop domain for activating the substrate and an oxygen-labile [4Fe-4S] cluster, while TtuB is a sulfur transfer protein with a thiocarboxylate C terminus (28). The structure of the TtuA holoprotein in the presence of an ATP analog confirmed the presence of a [4Fe-4S] cluster bound by three cysteine residues and demonstrated the nucleotide was positioned nearby. Furthermore, the structure of a TtuA–TtuB complex revealed the close juxtaposition of the TtuB thiocarboxylate with the open coordination site on the [4Fe-4S] cluster (27). These authors proposed a model in which the TtuB thiocarboxylate donates its sulfide to the [4Fe-4S] cluster, with the noncuboidal sulfide then attacking the activated substrate. Direct structural evidence for an extra-cubane sulfide bound to a [4Fe-4S] cluster was obtained for TtuA from *Pyrococcus horikoshii* (26). That enzyme uses inorganic sulfide (abundant in this microorganism's environment) as the sulfur source, rather than thiocarboxylated TtuB. Similar reactions are also likely to be used by TtuA from *T. maritima* (26), 2-thiouridine synthases of *T. thermophilus* (14) and *E. coli* (35), and probably by a broad range of other related enzymes (11, 14). Overall, the thionucleotide biosynthesis literature provides important precedents for the proposed mechanism of LarE_{Tm} involving interconversions between [4Fe-4S] and [4Fe-5S] states.

Experimental procedures

Vector construction and mutagenesis

Plasmid pET:LarE encoding the C-terminal His_6-tagged form of LarE from *T. maritima* was obtained from Prof. Tom Desmet. Codon-optimized *larE* was synthesized by GeneArt Gene Synthesis (Thermo Fisher Scientific) and subcloned into the pET21 vector at the NdeI and XhoI restriction sites. Site-directed mutagenesis was carried out using the gap-repair method (36) with mutations confirmed by sequence analysis. The pET:LarE plasmid and its derivatives were transformed into *E. coli* BL21 (DE3). The strains, primers, and plasmids used in this study are summarized in Table 1. The C172A/C92A, C172A/C95A, and C172A/C92A/C95A variants were created using the C172A plasmid with the C92A, C95A, and C92A/95A forward and reverse primers, respectively.

LarE_{Tm} purification

For aerobic purification of His_6-tagged LarE_{Tm}, *E. coli* BL21 (DE3) [pET:LarE] cells were grown in LB–Lennox medium supplemented with 100 mg/L carbenicillin at 37 °C with shaking at 225 RPM until reaching an OD_{600} of 0.5 to 1.0. The cells were induced with 0.4 mM IPTG and growth was continued for another 3 h at 37 °C with shaking. Cultures were harvested by centrifugation at 11,000*g* for 10 min, and cell pellets were stored at −80 °C until further use. The *E. coli* cell pellets were resuspended in 100 mM Tris–HCl, pH 7.2, buffer containing 300 mM NaCl, 5 to 10 mM 2-mercaptoethanol (βME), 2 mM phenylmethylsulfonyl fluoride, and 1 U/ml of Benzonase (EMD). The suspended cells were lysed using a French pressure cell at 16,000 psi and 4 °C. Cell-free lysates were obtained by centrifugation at 100,000*g* for 1 h and 4 °C. The lysates were loaded onto HisPur nickel-nitrilotriacetic acid resin (Thermo Fisher) that was equilibrated in 100 mM

Table 1
Strains, plasmids, and primers used in this study

Strain, plasmid, or primer	Characteristics or sequences	Description
Strains		
E. coli		
DH5α	F– Φ80lacZΔ M15 Δ (*lacZYA-argF*) U169 *recA1 endA1 hsdR17* (rK– mK+) *phoA supE44* λ- *thi–1 gyrA96 relA1*	Thermo Fisher
BL21 (DE3)	fhuA2 [lon] ompT gal (λ DE3) [dcm] ΔhsdS λ DE3 = λ sBamHIo ΔEcoRI-B int::(lacI::PlacUV5::T7 gene1) i21 Δnin5	NEB
Plasmids		
pET:LarE	Amp^r, pET21b with a 0.83-kb insert containing *larE* translationally fused to DNA encoding the 6x-His tag	
Primers		
LarE C92A-F	CCGCCTGATCGTGCCTATCTGTGTCGTAAACTGCGT	Gap Repair
LarE C92A-R	ACGATCAGGCGGATTTTCAATCAG	Gap Repair
LarE C95A-F	GATCGTTGTTATCTGGCCCGTAAACTGCGTGATAAC	Gap Repair
LarE C95A-R	CAGATAACAACGATCAGGCGG	Gap Repair
LarE C172A-F	GGATAAACCGGCAATGGCAGCCCTGTGTAGCCGTTTT	Gap Repair
LarE C172A-R	TGCCATTGCCGGTTTATCCCAGG	Gap Repair
LarE C174A-F	CCGGCAATGGCATGTCTGGCCAGCCGTTTT	Gap Repair
LarE C174A-R	CAGACATGCCATTGCCGGTTTATCCC	Gap Repair
LarE C172A/-C174A-F	GGATAAACCGGCAATGGCAGCCCTGGCCAGCCGTTTT	Gap Repair
LarE C172A/-C174A-R	CAGGGCTGCCATTGCCGGTTTATCCCAGG	Gap Repair
LarE C92A/-C95A-F	CCGCCTGATCGTGCCTATCTGGCCCGTAAACTGCGT	Gap Repair
LarE C92A/-C95A-R	ACGATCAGGCGGATTTTCAATCAG	Gap Repair

Tris–HCl, pH 7.2, buffer containing 300 mM NaCl using gravity flow at 4 °C. His$_6$-tagged LarE$_{Tm}$ was eluted from the column by stepwise increases in the concentration of imidazole (5, 20, 50, 100, then 350 mM imidazole) in some cases containing 5 to 10 mM βME. The homogeneity of the purified protein was checked by 12% SDS-PAGE. Protein concentrations were measured based on the absorbance at 280 nm (the His$_6$-tagged LarE$_{Tm}$ subunit has a calculated extinction coefficient at 280 nm of 24,200 M^{-1} cm^{-1}) (https://web.expasy.org/protparam/) or by using the Bradford reagent (Bio-Rad). The variants of His$_6$-tagged LarE$_{Tm}$ were purified using the same conditions as those for the WT enzyme.

Anoxic samples of His$_6$-tagged LarE$_{Tm}$ were purified from 0.3 l of aerobically grown *E. coli* cultures supplemented with 200 μM ammonium ferric citrate and 25 μM L-methionine (37) within an anaerobic chamber (Coy Laboratory Products) that contained an atmosphere of 95% N$_2$ plus 5% H$_2$ (<2 ppm [O$_2$]) and a palladium catalyst. The cells were lysed by addition of 0.2 to 0.3 mg/ml lysozyme, followed by incubation at 37 ℃ for 1 h. Cell-free lysates were obtained by centrifugation at 13,800*g* for 1 h at RT. Chromatography of the lysates was performed as described previously but inside the chamber at RT. All buffers used for the purification were degassed and allowed to equilibrate in the anaerobic atmosphere for at least 3 days prior to use.

For anaerobic growth, *E. coli* cells were cultivated in LB broth (Miller medium from NEOGEN Culture Media) supplemented with 0.5% w/v glucose, 100 mM Mops/NaOH, pH 7.4, 50 μg/ml carbenicillin, and 2 mM ferric ammonium citrate. The cultures were first grown aerobically at 25 ℃ until reaching an OD$_{600}$ of ∼0.7, then bubbled with Ar gas for 15 min and immediately moved into the anaerobic chamber. The anoxic medium for each sample was adjusted to contain 2 mM L-methionine, 2 mM L-cysteine, 25 mM sodium fumarate, and 0.5 mM IPTG (38). The containers were tightly sealed with parafilm and closed with GL-45 Pyrex caps. The cultures were grown anaerobically at 25 ℃ with minimum or no shaking for another 16 to 24 h, returned to the anaerobic chamber, transferred into centrifugal tubes, and harvested by centrifugation. The cell pellets were disrupted and LarE was purified inside the anaerobic chamber as mentioned previously

Assembly of the LarE$_{Tm}$ iron–sulfur cluster

Using anoxic buffer solutions within the anaerobic glove box, samples of His$_6$-tagged LarE$_{Tm}$ (previously purified using aerobic or anaerobic conditions) were incubated for 10 min at RT with DTT (at 50-fold concentration over the enzyme), followed by addition of 10 mM L-cysteine and His$_6$-tagged IscS$_{Ec}$ (used at 1/50th the amount of LarE$_{Tm}$), then incubated for 20 min. Subsequently, a 10-fold molar excess of FeCl$_3$ was slowly added, and the samples were incubated for 3 h at RT. Excess FeCl$_3$ and L-cysteine were removed using PD-10 desalting columns (GE Healthcare) that were equilibrated with 100 mM Tris–HCl, pH 7.2, buffer containing 300 mM NaCl. For chemical assembly of the iron-sulfur cluster, His$_6$-tagged LarE$_{Tm}$ was incubated with a 50-fold molar excess of DTT for 1 h, then slowly adjusted to have a 10-fold molar excess of FeCl$_3$, followed by addition of a 10-fold molar excess of freshly prepared Na$_2$S, and incubated for another 3 h inside the anaerobic chamber. The excess reagents for both methods were removed by passing the mixtures through PD MiniTrap G-25 columns (GE Healthcare) that were pre-equilibrated with 100 mM Tris–HCl (pH 7.2) buffer containing 0.3 M NaCl. The resulting LarE$_{Tm}$ holoprotein samples were concentrated using 10 kDa cutoff Amicon Ultra filters (Merck–Millipore) at RT. All of the samples were stored at RT and kept anoxic in an anaerobic glove box.

Purification of additional proteins

LarA, LarB, LarE, and LarC from *L. plantarum* (LarA$_{Lp}$, LarB$_{Lp}$, LarE$_{Lp}$, and LarC$_{Lp}$, respectively), LarA$_{Tt}$ apoprotein, and His$_6$-tagged IscS$_{Ec}$ were purified as previously described (4, 6–8, 10, 39).

Physical characterization of LarE$_{Tm}$ and IscS$_{Ec}$

To determine the subunit sizes of His$_6$-tagged LarE$_{Tm}$ and IscS$_{Ec}$ samples and to examine the sulfane sulfur content of IscS$_{Ec}$, protein samples (10–20 μM depending on the experiment) were injected onto a cyano-chemistry HPLC column that was equilibrated in 0.1% formic acid and eluted with an increasing gradient of acetonitrile. The fractions were analyzed by ESI-MS using a XEVO G2-XS instrument in positive ionization mode. The protein masses were derived from the MS data using MaxEnt (Waters Corp).

The native size of His$_6$-tagged LarE$_{Tm}$ was determined by size-exclusion chromatography using a Superdex 200 Increase 10/300 GL column equilibrated in 100 mM Tris–HCl, pH 7.2, buffer containing 300 mM NaCl at a flow rate of 0.5 ml/min, followed by particulate removal using a 0.2 μm filter that was placed in line with a miniDAWN TREOS multiangle light scattering detector and T-rEX refractive index meter (Wyatt Technology). The data were processed using ASTRA (Wyatt).

Native nano–ESI-MS of LarE$_{Tm}$ was performed using a Q Exactive UHMR instrument with a flow of nitrogen gas inside the sample holder so that samples were maintained under an anoxic atmosphere during the experiment. This was achieved by setting the sheath gas, auxiliary gas flow, and sweep gas flow to 4 (arbitrary units). Other instrumental parameters include capillary temperature of 250 °C, resolution of 12,500, C-trap pressure of 2, ion transfer m/z optimization set to high m/z, in-source trapping set to on, desolvation voltage of −150 V, detector m/z optimization set to low m/z, extended trapping of 50 eV, and, when optimizing monomeric species, applying an in-source CID of 100 eV. Data were collected over a broad m/z range (500–4000 m/z). Signals of sufficient signal-to-noise ratio were identified based on LarE mass calculations (Tables S1 and S2) accounting for an expected mass measurement accuracy of 10 ppm. Furthermore, recorded isotope abundance profiles were compared to theoretical abundance profiles for Fe- and S-containing protein ions. Unidentified signals in our native MS likely correspond to buffer component LarE$_{Tm}$ adducts commonly observed in such data (40, 41).

LarE$_{Tm}$ enzyme activity

Two methods were used to assay the activity of His$_6$-tagged LarE$_{Tm}$. First, a previously described LC-ESI-MS procedure (5) was used to monitor (i) the loss of P2CMN (m/z = 378 eluting at 4.62 min), (ii) the generation P2TMN (m/z = 410, eluting at 4.94 min), and (iii) the intermediate PCTMN (m/z = 394, eluting after 4.78 min). Secondly, we used an indirect coupled assay that relied on the generation of Lar activity (5). LarB$_{Lp}$ (10 μm) was first mixed with NaAD (0.2 mM), ATP (2 mM), MgCl$_2$ (20 mM), and NaHCO$_3$ (50 mM) in Tris–HCl buffer (100 mm, pH 7) and incubated for at least 10 to 15 min. The resulting solution (containing P2CMN) was mixed with anoxic samples of His$_6$-tagged LarE$_{Tm}$ (degassed and maintained inside the anaerobic chamber for at least 1 day; variable concentrations were used depending on the experiment), incubated for the times indicated at RT, then heat treated at 80 °C for 10 min. The sample was centrifuged (20,000g for

5 min), and the supernatant (containing P2TMN) was incubated with an equal volume of a mixture of LarC$_{Lp}$ (2.5 μM), MgCl$_2$ (10 mM), βME (10 mM), and CTP (0.1 mM) in Mes buffer (100 mM, pH 6) for 1 h at RT. The reaction was stopped by heat treatment at 80 °C for 10 to 20 min followed by centrifugation (20,000g for 10 min). The solution (containing the synthesized NPN) was mixed with an equal volume of buffer containing L-lactate (45 mM) and LarA$_{Tt}$ apoprotein (0.8 μM) in Hepes buffer (100 mM, pH 7). The solution was incubated for 5 min at 50 °C and then stopped by heat treatment at 90 °C using a thermocycler. The resulting D-lactate concentration was measured using a D-lactic acid/L-lactic acid commercial test (Megazyme), as described previously (4). The absorbance of NADH was monitored at 340 nm with a Shimadzu spectrophotometer (model UV 2600).

Biophysical characterization of the metallocenter

The metal content of His$_6$-tagged LarE$_{Tm}$ was assessed by using ICP-OES. Samples were prepared by boiling for 1 h in 35% (w/v) nitric acid before analysis using a model 710 Varian ICP-OES. The amount of acid labile sulfide was determined as previously described (42), with all steps carried out inside of an anaerobic chamber.

The UV-vis spectra were recorded under anaerobic conditions using an Ocean Optics UV-vis spectrophotometer or with a Shimadzu spectrophotometer (model UV 2600) under aerobic conditions. The effect of oxygen on the sample was investigated by monitoring changes in the spectrum over time after aerobic exposure. To examine the effects of reductant on the chromophore, protein samples (in 100 mM Tris, pH 7.2, buffer containing 300 mM NaCl) were mixed in anaerobic conditions with at least a 10-fold molar excess of sodium dithionite and incubated for 5 to 10 min before recording the spectra.

For EPR analysis, His$_6$-tagged LarE$_{Tm}$ was purified from anaerobically grown cells, its cluster assembled, the protein concentrated up to 600 μM and adjusted to contain 10% glycerol, then frozen in liquid nitrogen. EPR data were collected on a Bruker E680X EPR spectrometer operating at X-band and equipped with a Bruker SHQ-E cavity. The sample temperature was poised at 10 K using an Oxford ESR-900 liquid helium cryostat and an ITC-503 temperature controller.

Data availability

All data are available within the article and its supporting information file. The data underlying this article will be shared on a reasonable basis by submitting a request to the corresponding author.

Spectrometry Research Technology Support Facility for MS training and interpretations.

Conflict of interest—The authors declare that they have no conflicts of interest with the contents of this article.

Abbreviations—The abbreviations used are: βME, 2-mercaptoethanol; CID, collision-induced dissociation; EPR, electron paramagnetic resonance; ESI-MS, electrospray ionization-MS; ICP-OES, inductively coupled plasma-optical emission spectroscopy; IscS$_{Ec}$, cysteine desulfurase from *Escherichia coli*; Lar, lactate racemase; LarE$_{Lp}$, LarE from *Lactobacillus plantarum*; LarE$_{Tm}$, LarE from *Thermotoga maritima*; LC, liquid chromatography; MS, mass spectrometry; NaAD, nicotinic acid adenine dinucleotide; NPN, nickel-pincer nucleotide; P2CMN, pyridinium-3,5-biscarboxylic acid mononucleotide; P2TMN, pyridinium-3,5-bisthiocarboxylic acid mononucleotide; PCTMN, pyridinium-3-carboxy-5-thiocarboxylic acid mononucleotide; UV-vis, UV-visible.

References

1. Martinez Cuesta, S., Rahman, S. A., and Thornton, J. M. (2016) Exploring the chemistry and evolution of the isomerases. *Proc. Natl. Acid. Sci. U. S. A.* **113**, 1796–1801
2. Desguin, B., Zhang, T., Soumillion, P., Hols, P., Hu, J., and Hausinger, R. P. (2015) A tethered niacin-derived pincer complex with a nickel-carbon bond in lactate racemase. *Science* **349**, 66–69
3. Desguin, B., Urdain-Arraiza, J., Da Costa, M., Fellner, M., Hu, J., Hausinger, R. P., *et al.* (2020) Uncovering a superfamily of nickel-dependent hydroxyacid racemases and epimerases. *Sci. Rep.* **10**, 18123
4. Desguin, B., Goffin, P., Viaene, E., Kleerebezem, M., Martin-Diaconescu, V., Maroney, M. J., *et al.* (2014) Lactate racemase is a nickel-dependent enzyme activated by a widespread maturation system. *Nat. Commun.* **5**, 3615
5. Desguin, B., Soumillion, P., Hols, P., and Hausinger, R. P. (2016) Nickel-pincer cofactor biosynthesis involves LarB-catalyzed pyridinium carboxylation and LarE-dependent sacrificial sulfur insertion. *Proc. Natl. Acid. Sci. U. S. A.* **113**, 5598–5603
6. Rankin, J. A., Chatterjee, S., Tariq, Z., Lagishetty, S., Desguin, B., Hu, J., *et al.* (2021) The LarB carboxylase/hydrolase forms a transient cysteinyl-pyridine intermediate during nickel-pincer nucleotide cofactor biosynthesis. *Proc. Natl. Acid. Sci. U. S. A.* **118**, e2106202118
7. Fellner, M., Desguin, B., Hausinger, R. P., and Hu, J. (2017) Structural insights into the catalytic mechanism of a sacrificial sulfur insertase of the N-type ATP pyrophosphatase family, LarE. *Proc. Natl. Acid. Sci. U. S. A.* **114**, 9074–9079
8. Desguin, B., Fellner, M., Riant, O., Hu, J., Hausinger, R. P., Hols, P., *et al.* (2018) Biosynthesis of the nickel-pincer nucleotide cofactor of lactate racemase requires a CTP-dependent cyclometallase. *J. Biol. Chem.* **293**, 12303–12317
9. Fellner, M., Hausinger, R. P., and Hu, J. (2018) A structural perspective on the PP-loop ATP pyrophosphatase family. *Crit. Rev. Biochem. Mol. Biol.* **53**, 607–622
10. Fellner, M., Rankin, J. A., Desguin, B., Hu, J., and Hausinger, R. P. (2018) Analysis of the active site cysteine residue of the sacrificial sulfur insertase LarE from *Lactobacillus plantarum*. *Biochemistry* **57**, 5513–5523
11. Bimai, O., Arragain, S., and Golinelli-Pimpaneau, B. (2020) Structure-based mechanistic insights into catalysis by tRNA thiolation enzymes. *Curr. Opin. Struct. Biol.* **65**, 69–78
12. Shigi, N. (2021) Biosynthesis and degradation of sulfur modifications in tRNAs. *Int. J. Mol. Sci.* **22**, 11937
13. Jumper, J., Evans, R., Pritzel, A., Green, T., Figurnov, M., Ronneberger, O., *et al.* (2021) Highly accurate protein structure prediction with AlphaFold. *Nature* **596**, 583–589
14. Shigi, N., Horitani, M., MiyauchiI, K., Suzuki, T., and Kuroki, M. (2020) An ancient type of MnmA protein is an iron–sulfur cluster-dependent sulfurtransferase for tRNA anticodons. *RNA* **26**, 240–250
15. Kûlzer, R., Pils, T., Kappl, R., Hûttermann, J., and Knappe, J. (1998) Reconstitution and characterization of the polynuclear iron-sulfur cluster in pyruvate formate-lyase-activating enzyme. Molecular properties of the holoenzyme form. *J. Biol. Chem.* **273**, 4897–4903
16. Lambeth, D. O., and Palmer, G. (1973) The kinetics and mechanism of reduction of electron transfer proteins and other compounds of biological interest by dithionite. *J. Biol. Chem.* **248**, 6095–6103
17. Yu, M. A., Egawa, T., Yeh, S.-R., Rousseau, D. L., and Gerfen, G. J. (2010) Characterization of ascorbyl and sulfur dioxide anion radicals trapped during the reaction of bovine cytochrome *c* oxidase with molecular oxygen. *J. Magn. Reson.* **203**, 213–219
18. Waterhouse, A., Bertoni, M., Bienert, S., Studer, G., Tauriello, G., Gumienny, R., *et al.* (2018) SWISS-MODEL: homology modelling of protein structures and complexes. *Nucl. Acids Res.* **46**, W296–W303
19. Mihara, H., and Esaki, N. (2002) Bacterial cysteine desulfurases: their function and mechanisms. *Appl. Microbiol. Biotechnol.* **60**, 12–23
20. Lauhon, C. T., and Kambampati, R. (2000) The iscS gene in *Escherichia coli* is required for the biosynthesis of 4-thiouridine, thiamin, and NAD. *J. Biol. Chem.* **275**, 20096–20103
21. Zheng, L., Cash, V. L., Flint, D. H., and Dean, D. R. (1998) Assembly of iron-sulfur clusters. Identification of an *iscSUA-hscBA-fdx* gene cluster from *Azotobacter vinelandii*. *J. Biol. Chem.* **273**, 13264–13272
22. Hidese, R., Mihara, H., and Esaki, N. (2011) Bacterial cysteine desulfurases: versatile key players in biosynthetic pathways of sulfur-containing biofactors. *Appl. Microbiol. Biotechnol.* **91**, 47–61
23. Smith, A. D., Agar, J. N., Johnson, K. A., Frazzon, J., Amster, J., Dean, D. R., *et al.* (2001) Sulfur transfer from IscS to IscU: the first step in iron-sulfur cluster biosynthesis. *J. Am. Chem. Soc.* **123**, 11103–11104
24. Eschweiler, J. D., Kerr, R., Rabuck-Gibbons, J., and Ruotolo, B. T. (2017) Sizing up protein–ligand complexes: the rise of structural mass spectrometry approaches in the pharmaceutical sciences. *Annu. Rev. Anal. Chem.* **10**, 25–44
25. Crack, J. C., and Le Brun, N. E. (2021) Native mass spectrometry of iron-sulfur proteins. *Meth. Mol. Biol.* **2353**, 231–258
26. Arragain, S., Bimai, O., Legrand, P., Caillat, S., Ravanat, J. L., Touati, N., *et al.* (2017) Nonredox thiolation in tRNA occurring *via* sulfur activation by a [4Fe-4S] cluster. *Proc. Natl. Acid. Sci. U. S. A.* **114**, 7355–7360
27. Chen, M., Ishizaka, M., Narai, S., Horitani, M., Shigi, N., Yao, M., *et al.* (2020) The [4Fe-4S] cluster of sulfurtransferase TtuA desulfurizes TtuB during tRNA modification in *Thermus thermophilus*. *Commun. Biol.* **3**, 168
28. Chen, M., Asai, S. I., Narai, S., Nambu, S., Omura, N., Sakaguchi, Y., *et al.* (2017) Biochemical and structural characterization of oxygen-sensitive 2-thiouridine synthesis catalyzed by an iron-sulfur protein TtuA. *Proc. Natl. Acid. Sci. U. S. A.* **114**, 4954–4959
29. Ueda, C., Langton, M., Chen, J., and Pandelia, M. E. (2022) The HBx protein from Hepatitis B Virus coordinates a redox-active Fe-S cluster. *J. Biol. Chem.* **298**, 101698

30. Cavuzic, M., and Liu, Y. (2017) Biosynthesis of sulfur-containing tRNA modifications: a comparison of bacterial, archaeal, and eukaryotic pathways. *Biomolecules* **7**, 27

31. Leimkuhler, S., Buhning, M., and Beilschmidt, L. (2017) Shared sulfur mobilization routes for tRNA thiolation and molybdenum cofactor biosynthesis in prokaryotes and eukaryotes. *Biomolecules* **7**, 5

32. Mueller, E. G. (2006) Trafficking in persulfides: delivering sulfur in biosynthetic pathways. *Nat. Chem. Biol.* **2**, 185–194

33. Bouvier, D., Labessan, N., Clemancey, M., Latour, J. M., Ravanat, J. L., Fontecave, M., *et al.* (2014) TtcA a new tRNA-thioltransferase with an Fe-S cluster. *Nucl. Acids Res.* **42**, 7960–7970

34. Liu, Y., Vinyard, D. J., Reesbeck, M. E., Suzuki, T., Manakongtreecheep, K., Holland, P. L., *et al.* (2016) A [3Fe-4S] cluster is required for tRNA thiolation in archaea and eukaryotes. *Proc. Natl. Acid. Sci. U. S. A.* **113**, 12703–12708

35. Zhou, J., Lenon, M., Ravanat, J. L., Touati, N., Velours, C., Podskoczyj, K., *et al.* (2021) Iron-sulfur biology invades tRNA modification: the case of U34 sulfuration. *Nucl. Acids Res.* **49**, 3997–4007

36. Garcia-Nafria, J., Watson, J. F., and Gregor, I. H. (2016) IVA cloning: a single-tube universal cloning system exploiting bacterial *in vivo* assembly. *Sci. Rep.* **6**, 27459

37. Stewart, M. Y. Y., Bush, M. J., Crack, J. C., Buttner, M. J., and Le Brun, N. E. (2020) Interaction of the Streptomyces Wbl protein WhiD with the principal sigma factor s^{HrdB} depends on the WhiD [4Fe-4S] cluster. *J. Biol. Chem.* **295**, 9752–9765

38. Kuchenreuther, J. M., Grady-Smith, C. S., Bingham, A. S., George, S. J., Cramer, S. P., and Swartz, J. R. (2010) High-yield expression of heterologous [FeFe] hydrogenases in *Escherichia coli*. *PLoS One* **5**, e15491

39. Mueller, E. G., Palenchar, P. M., and Buck, C. J. (2001) The role of the cysteine residues of ThiI in the generation of 4-thiouridine in tRNA. *J. Biol. Chem.* **276**, 33588–33595

40. Tamara, S., den Boer, M. A., and Heck, A. J. R. (2022) High-resolution native mass spectrometry. *Chem. Rev.* **122**, 7269–7326

41. Karch, K. R., Snyder, D. T., Harvey, S. R., and Wysocki, V. H. (2022) Native mass spectrometry: recent progress and remaining challenges. *Annu. Rev. Biophys.* **51**, 157–179

42. Gilboa-Garber, N. (1971) Direct spectrophotometric determination of inorganic sulfide in biological materials and in other complex mixtures. *Anal. Biochem.* **43**, 129–133

43. Corpet, F. (1988) Multiple sequence alignment with hierarchical clustering. *Nucl. Acids Res.* **16**, 10881–10890